THE AMERICAN SOCIETY OF MECHANICAL ENGINEERS
345 E. 47th St., New York, N.Y. 10017

95-GT-414

COMPUTATIONAL METHODS FOR MODELLING PORT FLOWS IN GAS-TURBINE COMBUSTORS

James J. McGuirk & Adrian Spencer

Department of Aeronautical and Automotive Engineering and Transport Studies
Loughborough University of Technology
Leicestershire, LE11 3TU
United Kingdom

ABSTRACT

The objective of the present paper is to describe a computational technique which has been developed to allow the detailed geometry of the air-admission ports to be included in computational fluid dynamic studies of gas-turbine combustors. As CFD modelling of combustors continues to improve, it is likely that it will become commonplace to consider complete geometry descriptions of combustors (i.e. external as well as internal) in associated flow calculations, rather than carry out separate calculations, as is more usual currently. It will therefore be both necessary and desirable to include in the calculation the various geometrical features used in port design to control air admission and overall flow splits, (e.g. radiused/plunged/chuted holes, splitter plates, etc.). This requires modifications to standard mesh generation practices which are outlined and demonstrated here. As an illustration of the success and capabilities of the current method, flow field calculations are presented which contrast the changes in flow-split (as a consequence of discharge coefficient changes) and flow-patterns which are predicted when port geometry is varied from a plain hole to a plunged/chuted hole typical of some current designs.

INTRODUCTION

Computational modelling of combustor systems is generally performed in two stages; firstly the external aerodynamics are considered, allowing the calculation of the mass flow splits into individual ports of the combustor. Secondly, the internal flow field is calculated, using the bulk jet inlet conditions found from the external model. The models employed for the external calculations are often empirically based, or use simple, one- or two-dimensional computational models, e.g. Adkins and Gueroui [1], Karki et al. [2]. Although these methods give an indication of the flow split between the primary, intermediate and dilution ports, they provide little detailed information about the jet properties as they enter the combustion chamber. Jet velocity profiles, jet entry angle profiles and jet turbulence levels will, however, all influence the internal flow field to some extent. It is often suspected that poor predictions of combustor exit temperature profiles are due to the unresolved jet properties used as inlet conditions. Indeed, the best predictions of such an important parameter as exit temperature pattern factor are usually gained only when test data (e.g. from five hole probe measurements) are used to specify the velocity field in the various combustor inlet streams (see Shyy et al. [3]).

In order to avoid this dependency on test data, it will be necessary to extend the area of CFD modelling to include the external flow within the annuli surrounding the flame tube and carry out coupled external/internal calculations. This will certainly increase the computational expense and has so far rarely been attempted; Manners [4] contains one of the few reported examples of conducting coupled internal/external calculations. It is clear that this is the only route which brings the prediction of flow split information into the CFD model and allows prediction of the detailed flow parameters over port entry areas which might influence jet trajectory. However, it must be realised that this may prove a challenging task. It is known from experimental evidence (e.g. Hay and Spencer [5]) that the discharge coefficients of holes are quite sensitive to small geometry changes, and this fact is plain to see in the wide variety of port shapes used in combustors. Indeed, the sensitivity of the flow to small details, and hence the flow-field variations which can possibly result, (particularly with small annulus heights), has often led to port designs which attempt to control the jet trajectory more closely, hence the use of chuted ports in some combustors. Nevertheless, there have been some apparently successful attempts to predict discharge coefficient variations by fitting CFD meshes to hole geometry (e.g. Wittig et al. [6]), although this has not been done in the context of

Presented at the International Gas Turbine and Aeroengine Congress and Exposition
Houston, Texas - June 5-8, 1995

combustor air-entry ports, and the length to diameter ratio of the geometries considered in [6] was sufficiently large (typically 3.0) to make these flows easier to predict than typical combustor port scenarios. It seems therefore timely to re-visit the question of describing air-entry port details within CFD models of combustors, and this is the topic discussed in the present paper.

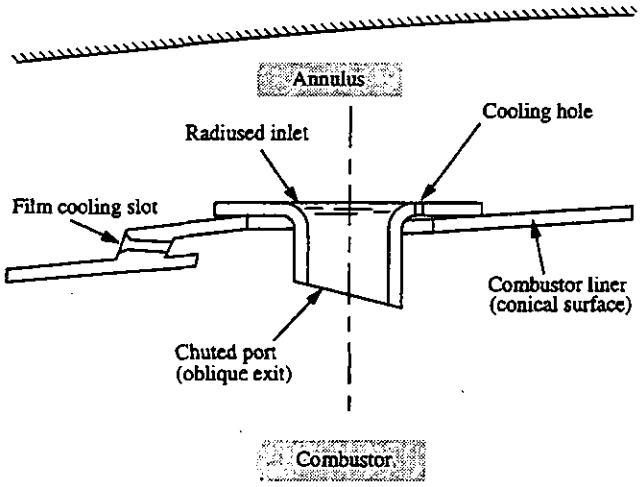

Figure 1. Typical port geometry

Combustor port geometry tends to be quite complex; an example is shown in figure 1. As mentioned above, this in itself is an indication of the importance of port flows and jet entry conditions, since it is as a consequence of wishing to fine-tune the jet flow characteristics that the complex port geometry arises during an iterative design and test cycle. Figure 1 shows a port comprising a chuted hole with inlet radiusing and oblique exit. The particular manufacturing method selected may produce a raised surface around the inlet to the hole, and small cooling holes may also be present immediately behind the chute. It would be impractical to model this level of detail using a single computational mesh given the number of admission ports in a typical combustor calculation, but it should be possible to improve upon the port representations used in current CFD predictions without significantly increasing the number of mesh cells required.

Shyy et al. [7] have described a method for generating curvilinear non-orthogonal body-fitted meshes for combustors which also allowed hole perimeter shape to be resolved. The generation scheme involved producing the mesh for the whole combustion chamber, then locally re-meshing areas around ports to form a port-fitted mesh. However, [7] performed only internal calculations, so this method only produced two-dimensional holes on the bounding surfaces of the solution domain. The methodology suggested in [7] has been extended and used by McGuirk and Spencer[8] to demonstrate the sensitivity of jet velocity profiles and annulus flow details to the hole description. The method was also demonstrated to be capable of predicting important differences in jet flow features (e.g. between round and 'D' shaped holes). This method has now been developed further such that three dimensional features can be represented within the computational grid. Three dimensional information will almost certainly be required for coupled internal/external calculations.

The following section details the steps required to modify a basic elliptic-equation-based mesh generator as typically used for combustors in order to allow the insertion of a module for locally fitting the mesh to as many details of port geometry as are desired to be resolved. When this method is combined with a flow solver, whose details are given briefly, CFD studies may be carried out to investigate the consequences of modifying port geometry. Results of CFD calculations for a plain round hole and an equivalent radiused/chuted geometry are then presented to indicate the capability of the present method in describing changes in discharge coefficient and jet flow patterns. The ability to conduct such calculations at an early stage in the combustor design cycle should prove most valuable.

GRID GENERATION

The basic concept which has been adopted in developing an air-admission port modelling facility is that a designer is likely to want to explore several modifications of port shape within the same basic combustor geometry. Accordingly, the present work has developed along the lines of providing a facility to include (and modify) the port geometry description within a given body-fitted mesh which characterises the internal and external space surrounding a given combustor liner. A module is provided to allow the user to re-mesh a portion of the original grid to form a boundary-conforming mesh which fits the locally distorted liner shape after inclusion of the port geometry. By storing the initial mesh it is possible to re-mesh port details and quickly generate a different port shape, thus providing a useful design tool. In what follows the various steps involved in the port modelling module are outlined.

Step 1

- *Generate a boundary conforming mesh which fits the combustor liner and outer casing shape, excluding all air-admission ports.*

Any desired method can be used to create an initial mesh which is fitted to the liner/casing geometry, but the method adopted in the present work has been to use the elliptic-pde method described by Thompson et al. [9], which involves solving a set of Poisson equations for the curvilinear co-ordinates:

$$\nabla^2 \xi^i = P^i$$

where $\xi^i = (\xi, \eta, \zeta)$ are the body-fitted curvilinear non-orthogonal co-ordinates. The actual problem solved is of course the inverse problem where the cartesian co-ordinates $r^i = (x, y, z)$ are solved for as dependent variables in the computational space defined by the curvilinear co-ordinates ξ^i as independent variables. The so-called control functions, $P^i = (P, Q, R)$, are used to control the spacing and orientation of the co-ordinate lines; for example these can be used to cluster grid lines near to the liner walls or in the region where the port is to be inserted to prevent too large distortions of the original mesh.

As an illustrative example, figure 2 shows a portion of a combustor liner (currently free of any primary air ports) and the mesh generated to fit to it using the above method.

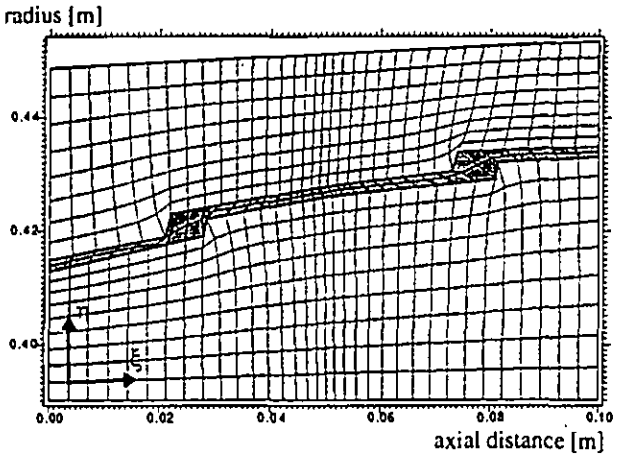

Figure 2. Mesh fitted to part of a combustor liner

Step 2

• *Provide a complete geometrical description of port.*

Clearly there are limits to the amount of information which can be resolved with the finite number of mesh nodes likely to be available to model each port. However, figure 3 indicates the type

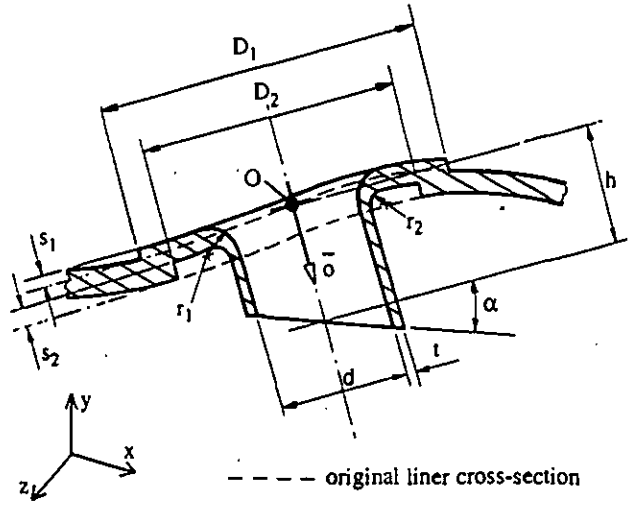

Figure 3. Port geometry definitions

and range of information which can be resolved in the current module. The extent to which this can model complete port geometries may be judged by comparing Figure 1 and Figure 3. Ten dimensions and two vectors fully define the geometrical details of the air-admission port, e.g.; position vector of centre of port (O), direction vector of the port axis($\bar{o}$), hole diameter (or other cross-sectional shape details) (d), chute thickness (t), chute height (h), exit plane angle (α) and internal and external fillet radii and platform heights and diameters (r_1,r_2,s_1,s_2,D_1,D_2). In addition to geometrical definition, this step also requires the user to specify a volume (defined by pairs of constant ξ, constant η and constant ζ planes) in the original mesh within which the re-meshing procedure will operate, leaving all other points of the original mesh unaltered. It is further necessary to specify the constant co-ordinate surfaces (i.e. two constant ξ,η or ζ planes) which define the inner and outer liner surfaces in the original mesh, and a third co-ordinate surface from the same family which will eventually be fitted to the exit plane of the chute. Finally, the number of mesh lines in the two spatial co-ordinate directions which lie in the liner surface and which define the resolution of the port are specified, (e.g. m×n cells which will cover the hole area).

Step 3

• *Move appropriate mesh nodes to resolve chute details fully.*

The cross sectional profiles defining the inner and outer shapes of the chute (e.g. two concentric circles for a round chuted hole) are calculated, using the geometrical details specified in step 2. and projected onto the upper (inner shape) and lower (outer shape) mesh surfaces defining the liner (projection taking place along the port axis direction vector, figure 3). The same profiles are also projected onto the chute exit plane, such that the inner and outer surfaces of the chute are now defined by the two cylinders joining the inlet and exit shapes. These projected profiles are used to choose the nearest mesh nodes in the original mesh (on the three selected surfaces as described above) which are then moved to lie on the projected profiles using the resolution specified in step 2. Interpolation between the mesh nodes defining the inlet and exit profiles of the chute, for both inner and outer shapes, allows all points on intermediate mesh surfaces to be located on the chute boundaries. At the end of this step the inside and outside chute surfaces (cylindrical in this example) have been defined with the required mesh resolution specified at step 2.

Step 4

• *Re-mesh liner surfaces to blend in changes to mesh made above.*

The 2 mesh planes defining the liner surfaces in the original mesh are now re-meshed so that points within these surfaces (and internal to the re-meshing volume defined in step 2) are moved into new positions to blend in the modifications in these mesh surfaces made in step 2. This re-meshing process consists of solving 2D elliptic pde's as specified above, but after each iteration the points are projected back onto the mesh surface as defined by the original grid. Thus liner surface mesh points are allowed to move around, but only within the original surface. This approach is simple and has been found to work well, but lacks robustness and further work is required to improve this. One such approach would be to replace the Laplacian operator with the Beltramian operator in the surface mesh generation scheme, as described by Warsi [10].

Step 5

• *Create fillet radii and platforms around chute as required.*

Small details of port geometry (e.g. inlet radiusing or a raised step on the outer liner wall) may be created by shifting discrete grid points in a direction parallel to the port-axis vector by specified amounts as given from the geometry information in step 2. Also at this penultimate stage some tidying up is necessary, e.g. for the points lying between the inner and outer diameters of the exit plane of the chute (for the case where several mesh lines are internal to the liner wall to resolve film-cooling flows or liner heat conduction processes). These are moved to lie within the surface defined by the chute exit plane, which is simply a matter of interpolation. At the end of this step all of the port geometrical features have been located with the selected resolution by moving all necessary points in the original mesh to lie on appropriate surfaces defining port inlet, exit and bounding planes. Figure 4 indicates an example of the distorted mesh at the end of this stage.

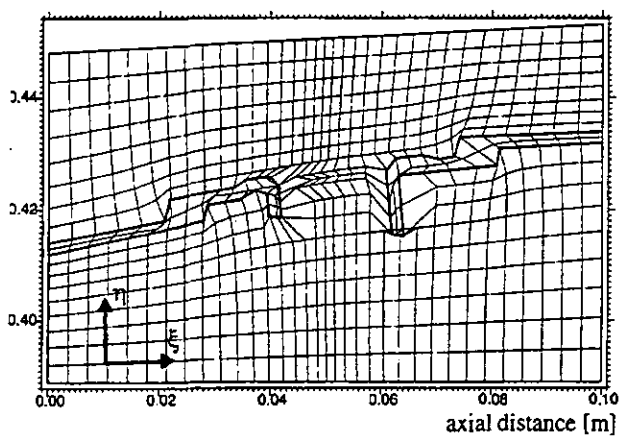

Figure 4. Mesh with all solid surfaces resolved

Step 6

• *Blend in all internal mesh nodes to fit the new surface and port definition.*

The final step is to re-solve the 3D Poisson equations within the selected volume to move the internal field mesh points to blend in with the changes made to the original mesh in steps 2-5. The control functions, P^i, calculated from the original mesh are used such that the original node clustering is retained.

Any number of ports may be introduced into a combustor liner or other solid surfaces by repeating steps 1-6. Figure 5 indicates the final liner and port-fitted mesh which results from the above procedure for a representative combustor geometry. The upper liner surface, and any mesh planes internal to the liner, are described by mesh planes similar to that in Figure 5(b), where the mesh plane contains a description of only the inner diameter of the chute. The lower liner surface, and any mesh planes used to describe the cross-section of the chute, are described by mesh planes similar to that shown in Figure 5(c) which contains a description of both inner and outer perimeters of the chute. It is by a stacking of these two styles of mesh planes (2 of 5(b) and 3 of 5(c) in this example) which makes up the third dimension of depth of the port, shown in cross-section in Figure 5(a). This grid is further illustrated in Figure 6 with a solid model of the geometry.

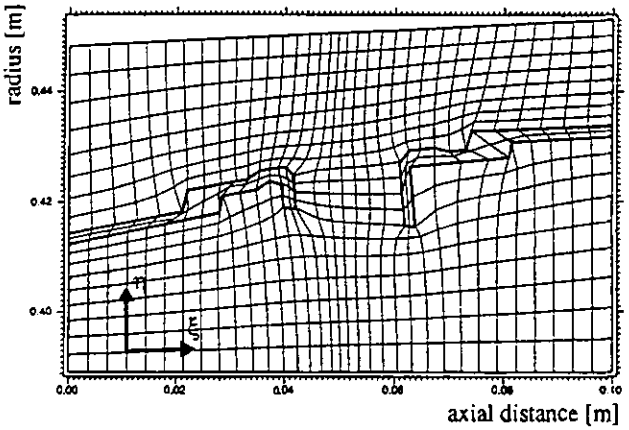

(a) cross-section through port, constant ζ-plane

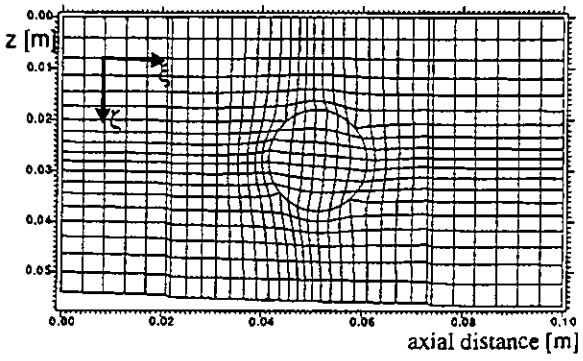

(b) upper liner surface defined by constant η-plane

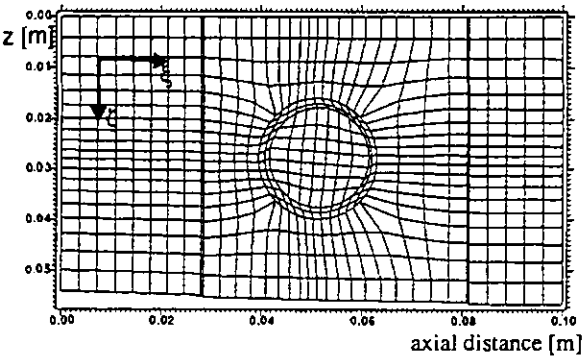

(c) lower liner surface defined by constant η-plane

Figure 5. Final liner and port fitted mesh

FLOW SOLVER

The CFD method used to solve for the flow on a mesh generated as described in the previous section is based on the isothermal, constant density, Reynolds-averaged form of the Navier-Stokes

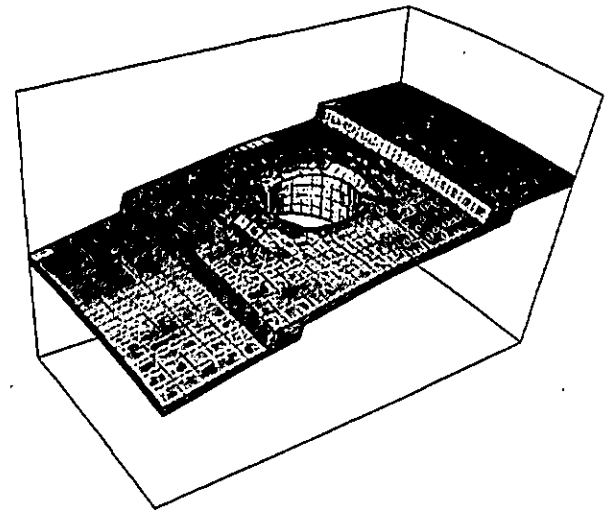

(a) upper liner surface

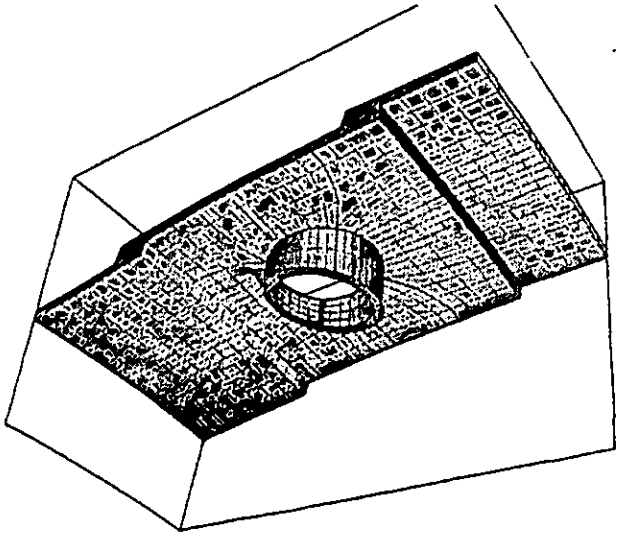

(b) lower liner surface

Figure 6. Solid model

equations, since, for the present purposes, only combustor aerodynamics is of interest and not reacting flow. The turbulence model used is the standard k-ε eddy viscosity model [11].

A cell-centred finite-volume scheme is used to discretise the equations where the convective discretisation follows either the HYBRID (upwind/central) scheme or the QUICK scheme. The SIMPLE pressure-correction method of Patankar and Spalding [12] was used to solve the equations, making use of the pressure-smoothing approach of Rhie and Chow [13] to avoid pressure-velocity uncoupling.

The code used is essentially the same code as used in previous studies of annulus/port flows [8], and is the same code as originally developed for the dump diffuser aerodynamics work of Little and Mannners [14].

TEST PROBLEM

In order to illustrate the ability of the port modelling method described here, a simple test problem has been devised. The geometry of this test problem is shown in Figure 7 and consists of parallel annulus and core flows. The axial velocities of the flow entering the annulus and core region were set to 40.0 and 12.0 m/s respectively, and a small bleed flow of 5.0 m/s was also specified at exit to the annulus. At the exit to the core, a zero gradient boundary condition is imposed on all solution variables normal to the exit plane, allowing an exit velocity profile to develop. The liner surfaces and the outer annulus casing were defined as walls with no slip (wall function) conditions, and the remaining 3 bounding surfaces of the computational domain were defined to be symmetry planes as indicated in Figure 7.

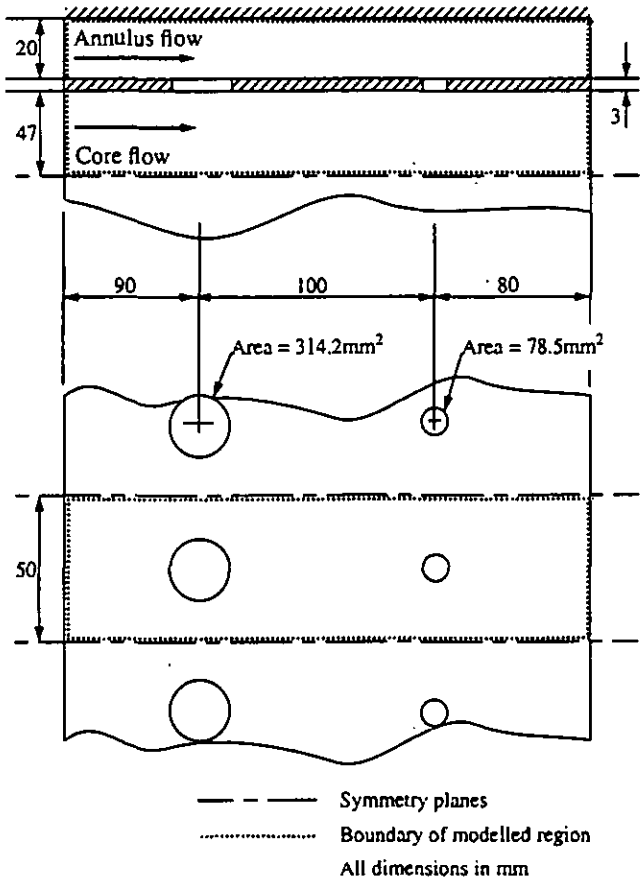

Figure 7. Test problem geometry

The annulus flow can enter the core flow via two rows of ports drilled in the liner with diameters chosen to give the hole plan areas as shown in Figure 7. Initially both ports are represented by plain holes and calculations are carried out for this geometry with the boundary conditions described above.

Subsequently a chuted hole is substituted for the plain hole of the upstream port. The chute used has a depth of 0.75 hole diameters, a thickness of 2mm, an inlet radius of 2mm and an exit plane angle, α, of 15 degrees. Using the same boundary conditions as above, the calculations are repeated to investigate the change in

flow split between the ports (caused by the change in discharge coefficient of the upstream port), changes in the flow and turbulence field etc. To carry out this illustrative comparison a mesh of 60×40×30 nodes in the ξ,η and ζ directions is used. Within this mesh 10×11 nodes are used in the plane of the first port opening and 5×6 nodes resolve the second, fixed port. These port resolutions were chosen to be comparable to those used in typical combustor flow calculations.

RESULTS

Figure 8 visualises the flow patterns obtained for the plain and chuted port designs using particle path streaklines and focusing attention in the vicinity of the upstream port. Noticeable changes have been brought about in the jet trajectory with more vertical jet penetration resulting from the chuted design, as expected. This leads of course to a stronger impingement process and therefore an enlarged upstream penetration of the fluid. For the conditions chosen only a small upstream vortex is obtained, but this has increased in both axial and vertical extent with the chuted port. The vena-contracta effect is also more visible in the plain hole than with the chuted geometry.

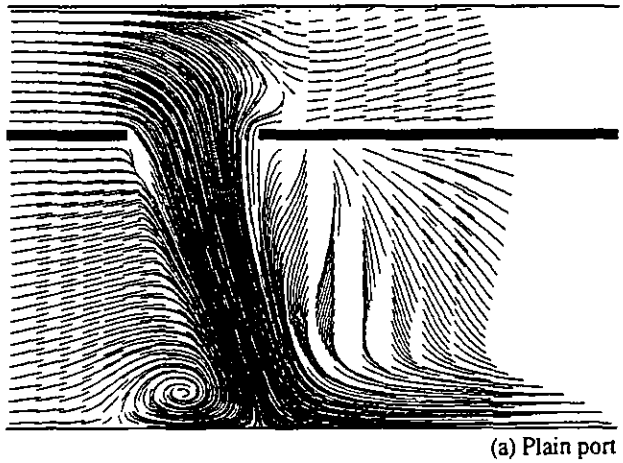

(a) Plain port

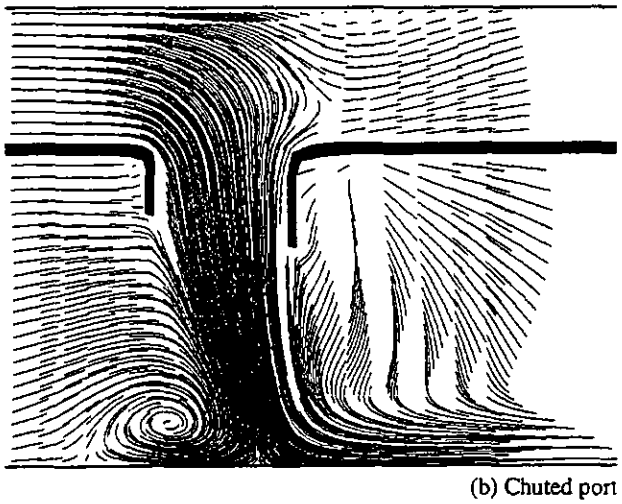

(b) Chuted port

Figure 8. Particle paths on plane through port diameter

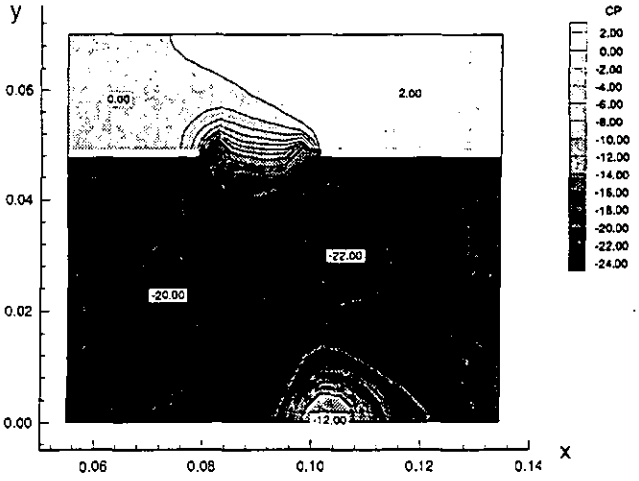

Figure 9. Pressure coefficient contours for plain port

Figure 9 shows the pressure distribution around the plain port ($C_p = (p_{ann} - p) / (0.5\rho U_{ann}^2)$). It can be seen that apart from the pressure gradient region accross the port and the impingement region where some pressure is recovered, the pressure field is quite uniform. To calculate the C_d for each port the pressure difference across the liner was evaluated. This was done by calculating the mass weighted total pressure in the annulus and the mass weighted static pressure in the core just upstream of each port. The ideal mass flow through each port could then be calculated from; $m_i = A_h\sqrt{2\rho\,(P_a - p_c)}$. By comparing this with the actual mass flow through the port its discharge coefficient was then obtained via; $C_d = \dot{m}_a / \dot{m}_i$.

To quantify the effect on jet exit angle, Figure 10 shows the predicted flow angle at the port exit for the two cases considered. In the chuted design the exit angle lies between 80° and 90° for all points except one at the upstream edge, whereas for the plain hole the angle exceeds 80° only at the furthest downstream point and values as low as 60° are observed.

Quantitative assessment of the changed flow pattern is given in Figures 11 and 12 in terms of impingement plane profiles of axial velocity and turbulence energy immediately below the port entry locations, both profiles being non-dimensionalised with the entry core flow velocity, U_c. The upstream shift of the recirculation zone ahead of jet impingement for the chuted port can be clearly seen, with the zero velocity location lying almost exactly on the port geometrical axis, further evidence of the improved vertical jet trajectory This change in jet trajectory has had an influence on the flow throughout the entire solution domain, and, because it also influences the flow split between the holes (as shown in Table 1), clearly changes the flow pattern in the vicinity of the second port quite dramatically. The stronger impingement of the chuted port increases the turbulence level generated, as well as shifting this upstream (see Figure 12), and the changed trajectory of the second jet has reduced the strength of impingement and hence associated turbulence production by about a factor of 2.

A comparison of bulk flow properties between the two test cases can be seen in Table 1. The predicted discharge coefficient

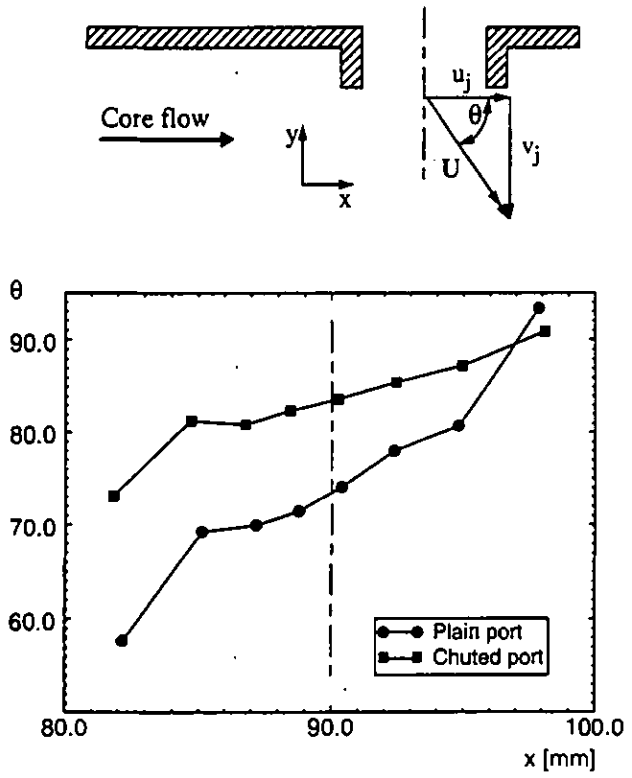

Figure 10. Definition and variation of flow angle at port exit

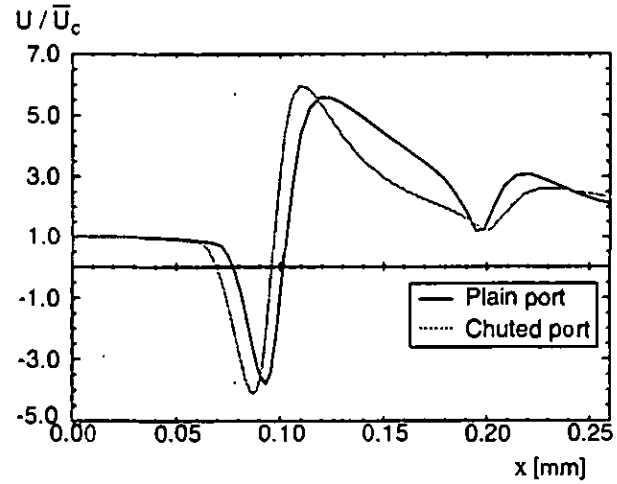

Figure 11. Axial velocity profile on plane of impingement

changes by 15% from 0.67 to 0.77 on changing from a plain to a chuted design. The latter is in excellent agreement with the experimental correlation given in Lefebvre [15] for plunged holes but the plain hole C_d is over predicted by some 15%. This is probably due to the presence of a vena-contracta effect in the plain hole flow pattern which influences the C_d value strongly; this has been noted by other authors [6] to be underpredicted by the k-ε turbulence model. The increase in C_d is accompanied by a shift of

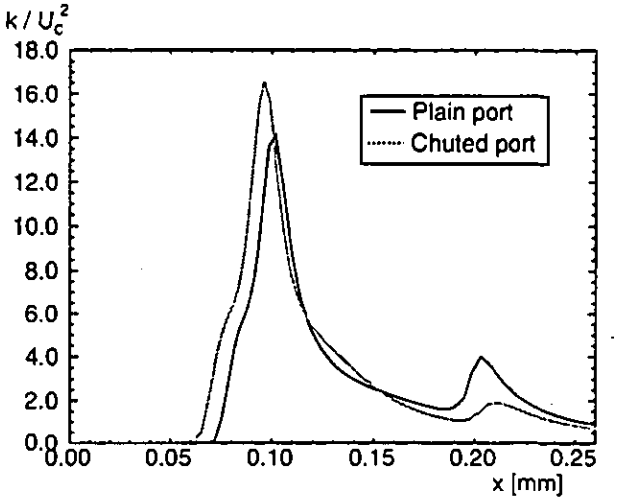

Figure 12. Turbulence intensity on impingement plane

mass flow to the first row of holes from the second and this leads to an increase in the effective jet/cross flow ratio ($\overline{V}_j$ / $\overline{U}_c$) from 7.31 to 7.53. The pressure loss (Δp^*) across the liner is also reduced by some 14% by moving to a chuted geometry. Finally, the mean jet angle averaged over the whole port area goes up from 76° to 89°, consistent with the profile information already presented in Figure 9. The mean jet exit angle for the plain port is in close agreement with the value of 72° obtained from the experimental correlation given in Adkins et al. [1], though no equivalent correlation is yet available for chuted ports

Table 1. Bulk flow properties of test cases

Parameter	Plain Port	Chuted port
C_d (prediction)	0.67	0.77
C_d (Lefebvre [15])	0.58	0.76
C_{d2} (Adkins [1])	0.59	-
$\dot{m}$ [kg/s]	0.0276	0.0284
$\overline{V}_j$ / $\overline{U}_c$	7.31	7.53
Δp^*	7.90%	6.63%
$\overline{\theta}$	76°	89°
$\overline{\theta}$ (Adkins [1])	72°	-
C_{d2} (prediction)	0.71	0.69
C_{d2} (Lefebvre [15])	0.62	0.62
C_{d2} (Adkins [1])	0.62	0.62
$\dot{m}_2$ [kg/s]	0.0074	0.0066

(Subscript 2 refers to downstream, plain port.)

CONCLUSIONS

A computational method has been described to enable detailed port shapes, typical of gas turbine combustors, to be included in CFD predictions of coupled internal and external combustor flows. The grid generation method is port geometry specific, allowing the user to describe the port geometry easily with few dimensions, hence modifications to a modelled port geometry can be made quickly. Since the grid defining all other combustor geometry (but excluding ports) is generated elsewhere, the initial grid needs generating only once. The initial grid can then be re-meshed to define any number of required ports. If a modification is then required to one of the port shapes, it may be done by recalling the original grid and passing it once more through the port mesh generating module. This procedure provides a valuable design tool in a "what if" type study on the effects of port position and shape changes. An example of the capability of this method has been presented in the current paper.

Using the flow solver described, a simple comparison between a plain hole and a chuted hole for an otherwise identical flow problem was performed. Substantial changes in the global and detailed flow field around the port were observed. The discharge coefficient of the port was seen to increase with the inclusion of the chute feature, as is found experimentally. Also apparent was a change in the port exit flow angle profile. Both of these effects lead to a significant change in the core flow field and turbulence levels, with obvious implications when solving for combusting flows.

ACKNOWLEDGEMENTS

This work has been carried out within the University Technology Centre in Combustor Aerodynamics at Loughborough University. The authors would like to acknowledge funding, support and useful discussions with colleagues at Loughborough, Rolls-Royce plc. and DRA (Pyestock).

REFERENCES

[1] Adkins, R.C. and Gueroui, D. (1986) "An Improved Method For Accurate Prediction Of Mass Flows Through Combustor Liner Holes." ASME Jnl. of Eng. For Gas Turbines and Power, Vol.108, pp491-497.

[2] Karki, K.C., Oechsle, V.L. and Mongia, H.C. (1990) "A Computational Procedure For Diffuser-Combustor Flow Interaction Analysis." ASME Paper 90-GT-35, 35th ASME IGTE, Brussels, Belgium.

[3] Shyy, W., Braaten, M.E. and Burrus, D. L. (1989) "Study of Three-Dimensional Gas-Turbine Combustor Flows", Int. Jnl. Heat and Mass Transfer, 32, pp 1155-1164.

[4] Manners, A. P. (1988) "The Calculation of Flow in Gas-Turbine Combustors", Ph.D. Thesis, Univ. of London.

[5] Hay, N. and Spencer, A. (1992) "Discharge Coefficients of Cooling Holes With Radiused and Chamfered Inlets", ASME Jnl. of Turbomachinery, 114, pp701-706.

[6] Wittig, S., Kim, S., Jakoby, R. and Weissart, I. (1994) "Experimental and Numerical Study of Orifice Discharge Coefficients in High Speed Rotating Disks", ASME Paper 94-GT-142, 39th ASME IGTE, The Hague, Netherlands.

[7] Shyy, W., Braaten, M.E. and Sober, J.S. (1987) "A Three-Dimensional Grid Generation Method For Gas-Turbine Combustor Flow Computations." AIAA Paper No. AIAA-87-0204, 25th Aerospace Sciences Meeting, Reno, USA.

[8] McGuirk, J.J. and Spencer, A. (1993) "CFD Modelling of Annulus Port Flows" ASME Paper 93-GT-185, 38th ASME IGTE, Cincinatti, Ohio.

[9] Thompson, J.F. Warsi, Z.U.A. and Mastin, C.W. (1985) "Numerical Grid Generation: Foundations and Applications." Oxford: North-Holland.

[10] Warsi, Z.U.A. and Tiran, W.N. (1986) "Surface Mesh Generation Using Elliptic Equations." Numerical Grid Generation in Computational Physics, Edited by J. Hauser and C. Taylor, Pineridge press, pp. 95-110.

[11] Jones, W.P. and Launder, B.E. (1973) "Prediction of Low Reynolds Number Phenomena With A Two Equation model Of Turbulence." Int. Jnl. Heat and Mass Transfer, 16, p1189.

[12] Patankar, S.V. and Spalding, D.B. (1972) "A Calculation Procedure for Heat, Mass and Momentum Transfer in Three-Dimensional Parabolic Flows." Int. Jnl. Heat and Mass Transfer, 15, p1787.

[13] Rhie, C.M. and Chow, W.L. (1982) "A Numerical Study of The Turbulent Flow Past an Isolated Airfoil." AIAA-82-0998.

[14] Little, A.R. and Manners, A.P. (1993) "Predictions of the Pressure Losses In 2D and 3D Model Dump Diffusers" ASME Paper 93-GT-184, 38th ASME IGTE, Cincinatti, Ohio.

[15] Lefebvre, A.W. (1983) "Gas Turbine Combustion" McGraw-Hill Series in Energy, Combustion and Environment.